INTERNATIONAL SOCIETY FOR SOIL MECHANICS AND GEOTECHNICAL ENGINEERING

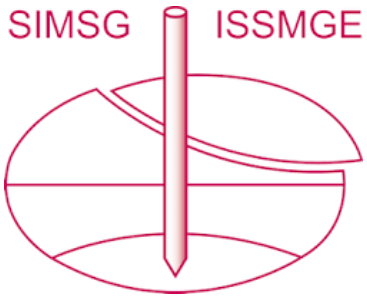

This paper was downloaded from the Online Library of the International Society for Soil Mechanics and Geotechnical Engineering (ISSMGE). The library is available here:

https://www.issmge.org/publications/online-library

This is an open-access database that archives thousands of papers published under the Auspices of the ISSMGE and maintained by the Innovation and Development Committee of ISSMGE.

The paper was published in the proceedings of the 10th European Conference on Numerical Methods in Geotechnical Engineering and was edited by Lidija Zdravkovic, Stavroula Kontoe, Aikaterini Tsiampousi and David Taborda. The conference was held from June 26th to June 28th 2023 at the Imperial College London, United Kingdom.

To see the complete list of papers in the proceedings visit the link below:

https://issmge.org/files/NUMGE2023-Preface.pdf

Proceedings 10th NUMGE 2023
10th European Conference on Numerical Methods in Geotechnical Engineering
Zdravkovic L, Kontoe S, Taborda DMG, Tsiampousi A (eds)

© Authors: All rights reserved, 2023
https://doi.org/10.53243/NUMGE2023-384

Seismic liquefaction potential assessment by means of automated numerical modelling

N. Tasso[1,2], M. Sottile[1,2], A. Sfriso[1,2]

[1]*SRK Consulting, Buenos Aires, Argentina*
[2]*Universidad de Buenos Aires, Buenos Aires, Argentina*

ABSTRACT: The state of the practice to evaluate the seismic liquefaction potential of a soil column entails the use of semiempirical methods that compare the cyclic stress ratio (CSR) with the cyclic resistance ratio (CRR). These methods are useful in practice because they are calibrated from limited real liquefaction cases, and are routinely employed although there is limited insight in the fundamentals behind them. In this work, a numerical modelling exercise is performed to determine which are the main aspects of the soil and the earthquakes that control the liquefaction phenomenon and understand why these methods work. A total of 6500 realizations of a soil column are performed, using the PM4Sand constitutive model implemented in Plaxis 2D. Real ground motion records are propagated through layers of liquefiable and non-liquefiable soils, and the results are compared with conventional linear and equivalent-linear site response analyses, in terms of PGA and CSR at the liquefiable layer. Finally, a discussion is presented regarding the predictive capability of the simplified methods and the value added by modern numerical modelling of soil liquefaction.

Keywords: Seismic liquefaction; Site-response analyses; Plaxis 2D; PM4Sand; Python

1 INTRODUCTION

The current practice for evaluating the susceptibility of soils to dynamic liquefaction involves a comparison of the Cyclic Stress Ratio (CSR) with the Cyclic Resistance Ratio (CRR). If the CSR exceeds the CRR during an earthquake, liquefaction is considered to occur. Being based on empirical data from sites where liquefaction has been observed, and having been successively refined along many years, these methods are now considered reliable and therefore routinely used in practice. However, they have limitations: i) the estimation of CSR involves non-linear correction coefficients that depend on the site and earthquake characteristics (Cetin et al, 2000) and which assume that pore pressures and liquefaction do not affect upwards wave propagation (Dobry, 2015); and ii) CRR is defined based on the relative density, and largely ignores many other relevant aspects of soil behaviour (Dobry, 2015).

Numerous studies have been conducted to understand key factors governing liquefaction during earthquakes, including non-linear site response analyses (Cetin et. al, 2000), Bayesian updates (Cetin et al., 2001) and machine learning techniques (e.g. Oommen et al., 2010; Zhang and Wang, 2020; Atangana et al., 2020). Most site response analysis methods incorporate site amplification but neglect the impact of the induced pore pressure on shear wave velocity and wave propagation (Dobry, 2015). Machine learning techniques, calibrated on real-world cases, are on the other hand the natural evolution of ad-hoc updates of current procedures.

In this paper, a numerical modelling exercise on wave propagation and liquefaction is presented. A 1D layered soil column of fixed height, containing one liquefiable layer of varying thickness and density, confined by two non-liquefiable layers, is built. This column is subjected to a large set of real ground motions, and the buildup of pore pressure is tracked in the liquefiable layer. Results are plotted in a $CSR - (N_1)_{60}$ chart, isoprobability curves are determined and are afterwards compared with the Idriss and Boulanger (2008) chart. This exercise, while preliminary and limited in scope, might provide support to the liquefaction charts used in practice.

2 REVIEW OF THE STATE OF PRACTICE

The first method for estimating the risk of liquefaction was proposed by Seed and Idriss (1971). In this method, CSR was defined in the first place, and CRR was estimated using SPT data. The method was later revised by Youd et al. (2001). Robertson (1998) and Boulanger and Idriss (2016) made analogous contributions where CPT data is employed.

CSR is defined as the ratio between the equivalent uniform shear stress (τ_c) during the earthquake and the pre-seismic vertical effective stress (σ'_{v0}). Seed and Idriss (1971) estimate τ_c as 65% of the max shear stress (τ_{max}) that occurs during an earthquake. The dependence of τ_{max} with depth is calculated from the Peak Ground Acceleration (PGA), the total vertical stress (σ_{v0}) and a depth correction coefficient (r_d).

Dobry and Abdoun (2015), and Youd et al. (2001), highlighted the limitations of the simplified method by Seed and Idriss (1971) . Those limitations can be summarized as follows: i) the factor 0.65 assumes that the non-uniform cyclic stresses that occur during an earthquake can be represented by a number of equivalent cycles of uniform cyclic stresses; ii) the depth correction coefficient has a strong non-linearity with respect to the soil and earthquake properties; iii) τ_{max} and PGA does not consider the impact of pore pressure build-up on the reduction of stiffness and strength of the liquefying layer. The latter drawback becomes critical when using site-response analyses, as it is equivalent to assuming that the degradation of the shear modulus (G/G_{max}) is the same before, during and after liquefaction (Dobry, 2015). Kramer (2019) illustrated that liquefaction has an important effect on the amplitude and frequency content of the seismic signal.

3 NUMERICAL ANALYSIS

3.1 Geometry and mesh

A plane-strain 1D soil column was modelled in Plaxis (2023). The column is $20\ m$ high, is divided in three layers (Figure 1): two non-liquefiable (HC: upper and HB: lower) layers with a relative density $D_r = 90\%$, and one liquefiable (HL: middle) layer with a variable density $35\% < D_r < 90\%$. The water table is fixed at the contact between HC and HL.

Forty 15-node elements were used to achieve a balance between computation speed and correct wave propagation before liquefaction. The bottom boundary is a compliant base, while the lateral sides entail tied degrees of freedom.

3.2 Constitutive models

Non-liquefiable layers HB and HC are modelled with the HSS model (Plaxis 2023). This model captures hysteretic damping, but cannot capture the generation of pore pressure due to cyclic loading. The reference stiffness at small strain (G_0^{ref}) was adopted as a function of D_r while the remaining stiffness parameters (E_{50}^{ref}, E_{oed}^{ref} and E_{ur}^{ref}) were determined from cascade correlations commonly used in practice. During the simulations, it is assumed that these materials do not generate excess pore pressures. Parameters are shown in Figure 1.

PM4Sand was selected to characterize the behaviour of the liquefiable layer HL. This model allows for a realistic simulation of the generation of pore pressure due to cyclic loading and its impact on shear stiffness, shear strength and wave propagation. The adopted parameters are also shown in Figure 1.

Similar to Bray and Macedo (2017), default parameters proposed by Ziotopolou and Boulanger (2015) were employed for the parameters of the model not shown in Figure 1.

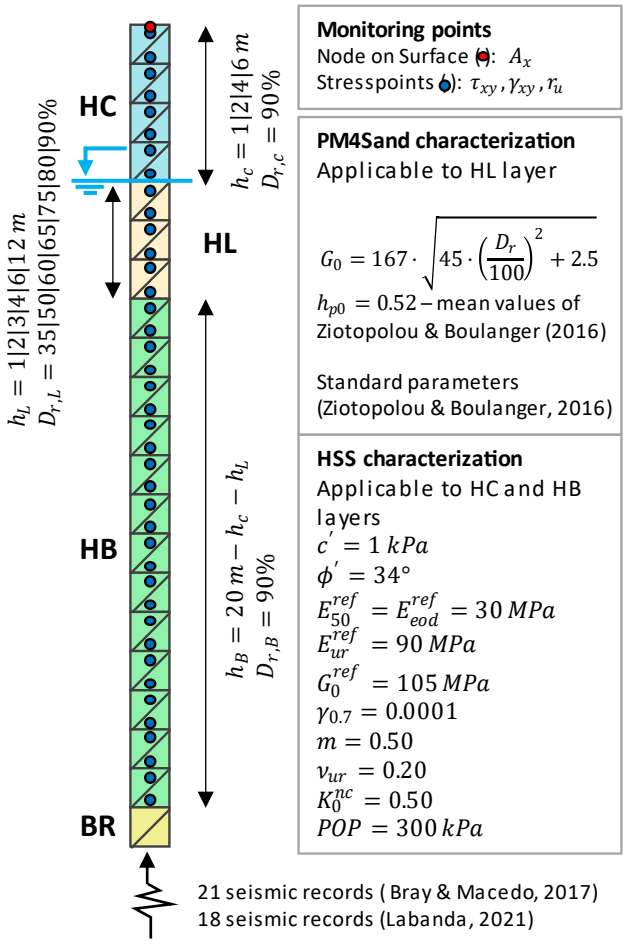

Figure 1: Geometry and mesh of the soil column and material parameters.

For a given value of the parameter h_{p0} and CSR, the number of cycles to liquefaction depends on D_r. In this study, a fixed value of h_{p0}, average of the values reported by Ziotopolou and Boulanger (2015) was used. However, the influence of h_{p0} in the number of cycles to liquefaction is large, and therefore further analysis is required to confirm the results presented in this study for other values of h_{p0}.

3.3 Seismic records

39 records from rock outcrops or firm soil sites, taken from the PEER NGA-West2 database were employed. 21 seismic records were inherited from Bray and Macedo (2017) and 18 from Labanda et al (2021). Ranges are: $PGA = 0.14|1.02\ g$, Arias Intensity $AI = 0.1|9.1\ m/s$, and significant duration $t_{5-95} = 5|41\ s$.

In order to optimize calculation times, the earthquakes were symmetrically trimmed while maintaining 96% of AI. A Hann window was used at each end of the signal, equivalent to 5% of the trimmed duration and a Butterwood filter of $0.05\ Hz$ was also applied. The signal processing technique recommended by Ancheta et al. (2014) was followed. The acceleration was then introduced into the compliant base of the model (Vilhar et al. 2018).

3.4 Realizations

The 39 seismic records were propagated through 168 FEM 1D columns, in turn obtained by swapping 4 depths, 6 thicknesses and 7 values for the relative density of the liquefiable (HL) layer, resulting in a total of 6552 realizations. A node on the surface was selected to study the evolution of a_{max}. Shear stress (τ_{xy}), shear strain (γ_{xy}) and pore pressure ratio (r_u) were recorded at 40 locations within the soil column.

The results were processed to determine the onset of liquefaction, defined using typical thresholds (e.g., Idriss, 2008): $\gamma_{xy} > 3\%$ or $r_u > 0.90$. The generation of the models, calculations, and post-processing were performed automatically using a Python script.

3.5 SRA analysis

The 6552 realizations were processed using the standard Site Response Analyses (SRA) commonly used in practice. Linear and equivalent-linear analyses implemented in the Python library pyStrata were employed. The first one is a linear analysis with a constant Rayleigh damping of 5% for all layers, while the second one uses a linear-equivalent formulation for the liquefiable layer which accounts for soil stiffness degradation and variable damping (Darendeli 2001) but fails short in accounting for the impact of pore pressure build-up on the propagation of mechanical waves through the soil column.

4 COMPARISON, FEM MODELS VS SRA

4.1 PGA

Figure 2 presents a comparison of the PGA at surface obtained through the 1D FEM simulations and the site response analyses SRA.

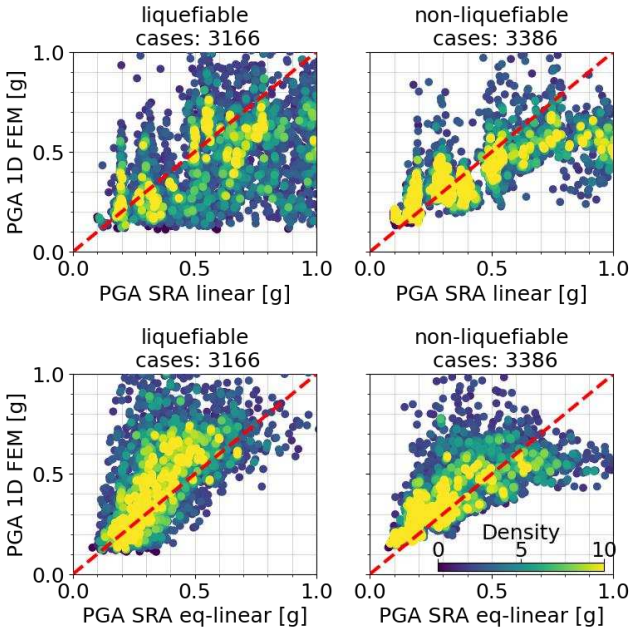

Figure 2: Comparison of PGA from FEM and SRA models for liquefiable (left) and non-liquefiable (right) cases.

Results are divided into cases where liquefaction was observed in the numerical models and where liquefaction was not triggered, and are shown independently for the linear and equivalent-linear SRA models.

When no liquefaction occurs, the difference between the two analyses is important but tolerable, and the bias is relatively small. When $PGA > 0.5g$, FEM simulations yield lower $PGAs$ than SRA for both the equivalent-linear and linear methods.

On the other hand, when liquefaction is observed, a strong bias and a large scatter between the FEM and SRA analyses is observed: the linear SRA shows no trend, while the equivalent-linear SRA shows a strong bias on the unconservative side. These observations seem to confirm the criticism by Dobry (2015): PGA estimated from SRA analyses does not properly account for the effect of liquefaction on wave propagation.

4.2 CSR

The evolution of shear stresses was recorded every $0.5\ m$ in both the FEM and SRA models. At each depth and in each case, the maximum shear stress (τ_{max}) was determined and a CSR (corrected for magnitude and confining pressure) was calculated according to Boulanger and Idriss (2016) (eqn. 1)

$$\mathrm{CSR}_{M=7.5|\sigma'_v=1\ atm} = \frac{0.65 \cdot \tau_{max}}{\sigma'_{v0} \cdot MSF \cdot K_\sigma} \qquad (1)$$

Figure 3 presents a comparison between the value of CSR obtained in the FEM and SRA models, for points within the liquefiable layer (HL) only. Again, results are divided into cases: with and without liquefaction observed in the numerical models.

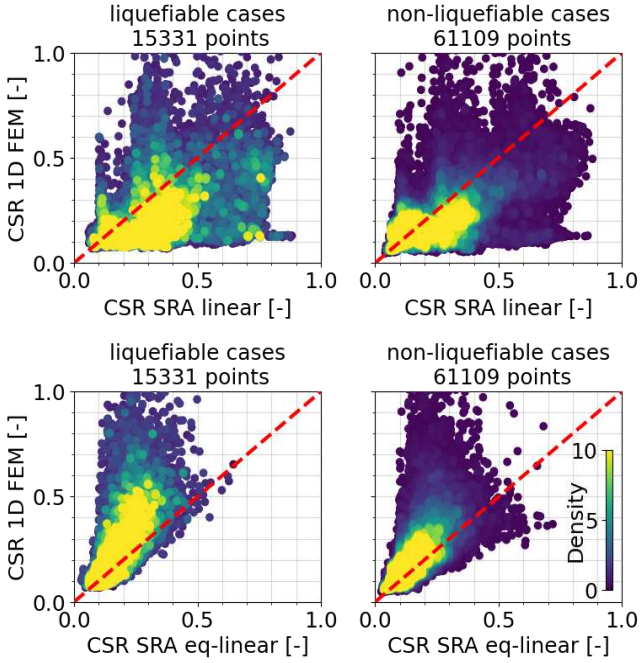

Figure 3: Comparison of CSR from FEM and SRA models for liquefiable (left) and non-liquefiable (right) cases.

Again, in the no liquefaction cases the difference between the FEM and equivalent-linear SRA analyses is high but tolerable and the bias is also moderate. The linear SRA has a strong bias and scatter, yielding it of little value for reliable practical applications. When liquefaction occurs, the linear SRA tends to overpredict CSR with a huge scatter, while the equivalent-linear SRA underpredicts CSR with a medium-to-high scatter.

It must be noted that the 1D FEM model can only simulate the liquefaction of an infinite horizontal layer. In real life, liquefiable soils at a given site may exist in continuous or discontinuous layers and pockets, and therefore caution must be exercised when extracting practical conclusions from the comparisons shown here.

4.3 Effect of relative density

Figure 4 presents a comparison of CSR – for points within HL – between the FEM models and the linear SRA. Results are grouped by relative density 35%, 60% and 80% (in the HL layer) and whether liquefaction occurred or not.

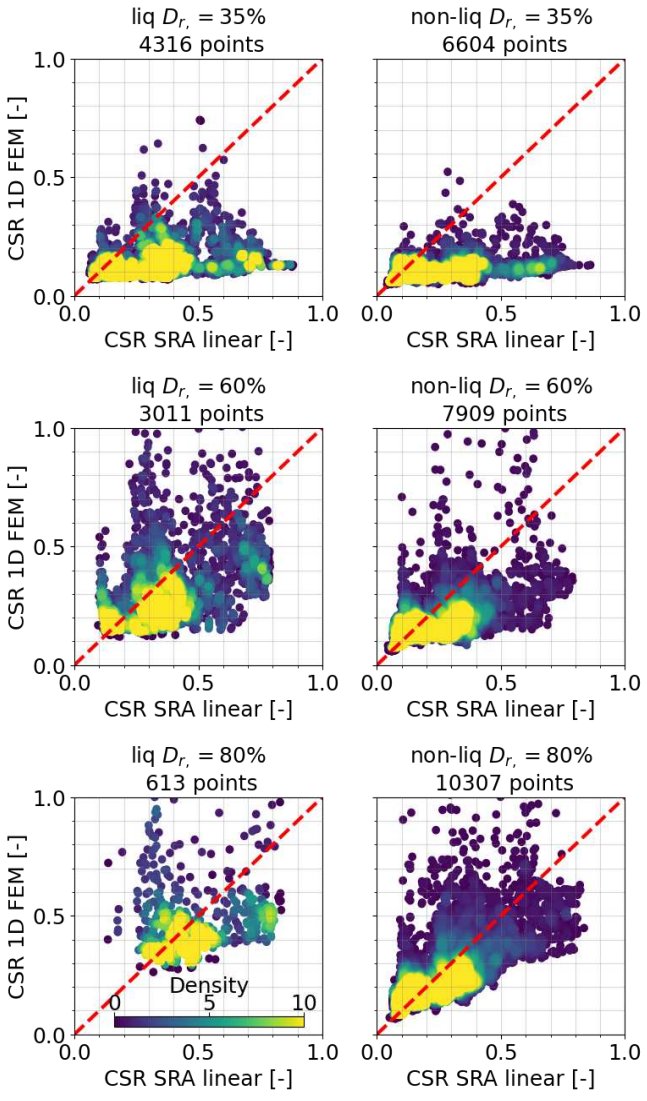

Figure 4: Comparison of CSR obtained from FEM and SRA models for liquefiable (left) and non-liquefiable (right) cases, separately by three selected relative densities.

SRA results for loose soils ($D_r = 35\%$) show much higher CSR values than the FEM models. One possible explanation is that the pore pressure generation in the FEM model attenuates the wave propagation and reduces τ_{max}. For denser soils ($D_r = 80\%$), the matching between FEM and linear SRA models improves, indicating that the latter is acceptable for dense soils when liquefaction is not of a concern.

Another interesting observation is that the CSR required to trigger liquefaction in the FEM models increases as the relative density increases. For $D_r = 35\%$, the threshold is $CSR = 0.05$, for $D_r = 60\%$ it is $CSR = 0.10$, and for $D_r = 80\%$, $CSR = 0.30$ is required to trigger liquefaction.

5 A COMPARISON WITH SEMIEMPIRICAL METHODS

The results obtained from FEM simulations and linear SRA analyses can be compared with the charts from the semiempirical methods used in practice. To achieve this, the relative density was converted to SPT blow-count according to Idriss (2008) (eqn. 2):

$$(\mathrm{N}_1)_{60} = 46 \cdot D_r^2 \qquad (2)$$

The CSR histograms were plotted for each relative density and separated into liquefaction (red) and non-liquefaction (green) in Figure 5. The probability of liquefaction was computed by dividing the number of cases where liquefaction was observed by the total number of cases within a limited win-dow of $(N_1)_{60}$ and CSR. Finally, iso-probability contours were plotted for linear SRA (left) and FEM simulations (right).

The CSR distribution histograms of the FEM model (Figure 5 right) show that liquefiable cases are mostly contained within the boundaries of the simplified methods. It is also observed that the magnitude of CSR decreases for liquefaction cases as it moves away from the liquefaction boundary. This suggests that once liquefaction occurs, it influences seismic wave propagation, attenuating it and preventing higher CSR values from being reached. These observations do not apply to the linear SRA, as high CSR values can be achieved even when liquefaction is expected because liquefaction does not change wave propagation in the SRA method.

A notable coincidence is observed between the iso-probability curves obtained and the shape and location of the liquefaction boundary for both methods. It is interesting to note that the probability of liquefaction associated with the boundary reported by Idriss and Boulanger (2008) using the FEM simulations is 15-20%. As this result comes from an inherently conservative 1D study that does not account for discontinuous liquefiable layers, it may mean that, while the boundaries defined by the simplified methods are effective, they are also somewhat conservative.

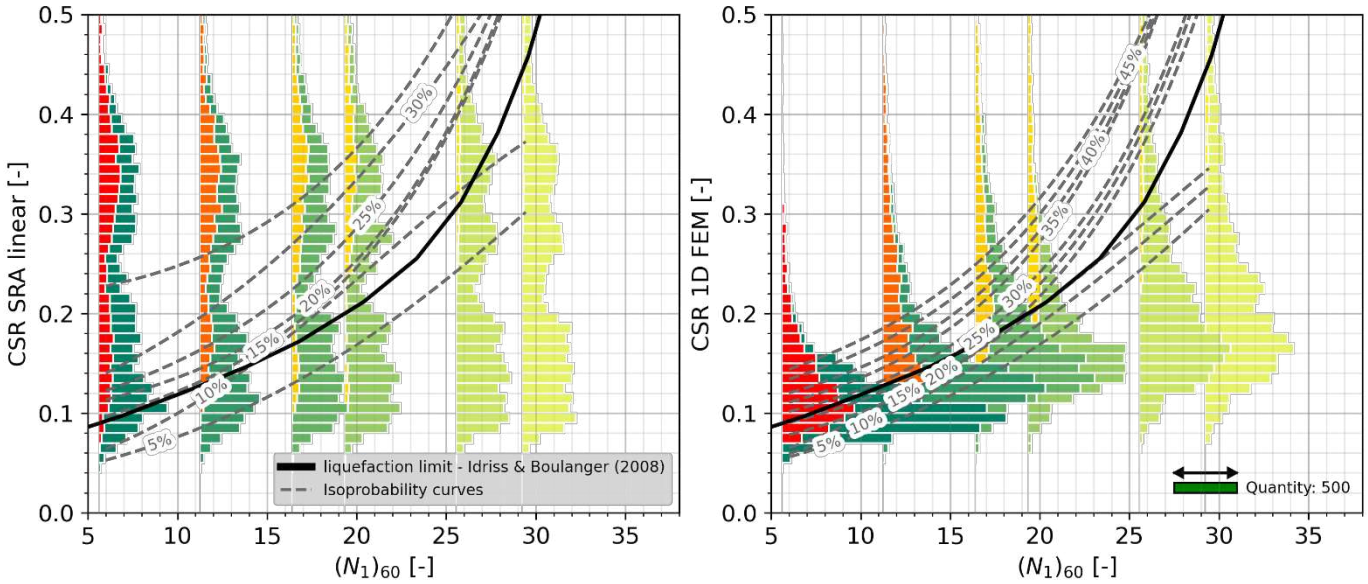

Figure 5:Threshold CSR for liquefaction, obtained from linear SRA (left) and FEM simulations (right). Histograms represent liquefaction (red) and non-liquefaction (green) cases.

In SRA simulations, the iso-probability curves are more widely separated due to the larger CSR values. and the probability associated with the liquefaction boundary ranges from 5-20%.

Figure 6 is a clean copy of Figure 5, and summarizes the findings of this study. In this figure, CSR should be computed with a linear SRA calculation, which is normal routine practice. Equivalent-linear SRA would provide a different chart with (maybe) a slightly better predictive capability. Of course, if numerical techniques like the 1D soil column shown here are employed, there is no need and value in using a chart like the one shown in Figure 6. Figure 6 updates the results of a previous work (Sottile et al. 2021).

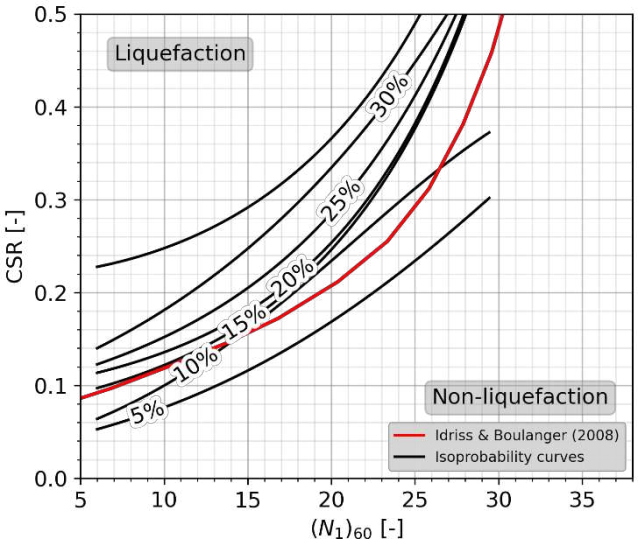

Figure 6: Isoprobability curves compared with the Idriss and Boulanger (2008) liquefaction boundary.

Again, it must be emphasized that the 1D FEM model employed in this study simulates one infinite horizontal layer of liquefiable ground. Interbedded stratigraphy and liquefiable pockets surrounded by non-liquefiable materials fall beyond the scope of this study. Also, the study must be repeated for other configurations, including other values of h_{p0}, varying parameters of the non liquefiable layers and other heights of the soil column. Therefore, the application in practice of the results shown in Figure 6 must be done with extreme caution.

6 CONCLUSIONS

Simplified methods for evaluating seismic liquefaction are reliable but have some limitations: i) they are based on limited real cases of site liquefaction where subsidence or surface material ejecta was observed; ii) the estimation of CSR includes depth correction factors that depend on site and seismic properties; iii) in computing CSR, it is assumed that pore pressure generation and eventual liquefaction do not affect wave propagation; and iv) CRR is defined based on relative density and ignores other aspects of soil behavior.

In this work, 6552 numerical simulations of a soil column were carried out; 39 real seismic records were put through 168 stratigraphies including liquefiable layers modelled by the PM4Sand constitutive model. Linear and linear-equivalent site response analyses were performed for the same conditions, and the results were compared for PGA, CSR and the effect of D_r.

The comparison between the FEM models and those based on SRA show that: i) liquefaction of the confined layer, by itself, has a notable effect on the value of PGA recorded at the surface of the numerical models, at least for the case of the 1D column; ii) pore-pressure induced changes in shear modulus produce a notable dispersion (scatter) in the value of CSR obtained by FEM models and SRA analyses measured within the liquefiable layer.

The results obtained from the numerical simulations were also compared with semiempirical methods. A notable coincidence was observed with respect to the shape and location of the liquefaction boundary of the simplified methods. The probability of liquefaction associated to the boundary reported by Idriss and Boulanger (2008) is typically 5-20%. Therefore, it is concluded that the boundaries defined by the simplified methods work, but may be slightly conservative. The scope of this numerical exercise, being 1D and therefore not accounting for discontinuous liquefiable layers, does not allow for conclusive results, nor does it provide enough elements to propose adjustments to the simplified methods that are the state of the practice.

Although this study provides valuable insights, it must be emphasized that a 1D column simulates one infinite horizontal layer of liquefiable ground, ignoring the effect of interbedded stratigraphy and liquefiable pockets surrounded by non-liquefiable materials which are frequent in real soil deposits. Also, the study must be repeated for other configurations, including other values of h_{p0}, varying parameters of the non liquefiable layers and other heights of the soil column. Therefore, the application in practice of the results of this study must be done with extreme caution.

7 ACKNOWLEDGEMENTS

The authors thank SRK Consulting for their financial support, and acknowledge the contributions, comments, and suggestions by their colleagues at SRK Consulting and at the University of Buenos Aires during this research.

8 REFERENCES

Ancheta, T., Darragh, R., Stewart, J., Seyhan, E., Chiou, W., Wooddell, K., Graves, R., Kottke, A., Boore, D., Kishida T., Donahue, J. 2013. *PEER NGA-West2 Database, PEER Report 2013-03*, University of California, Berkeley, CA.

Atangana, P.G., Shen, S.L., Zhou, A., Lyu, H. 2020. Evaluation of soil liquefaction using AI technology incorporating a coupled ENN / t-SNE model. *Soil Dynamics and Earthquake Engineering* **130**.

Boulanger, R., Idris, I.M. 2016. CPT-Based Liquefaction Triggering Procedure. *Journal of Geotechnical and Geoenvironmental Engineering, ASCE* **142**, 442-459.

Bray, J., Macedo, J. 2017. 6th Ishihara Lecture: Simplified procedure for estimating liquefaction induced building settlement. *Soil Dynamics and Earthquake Engineering* **102**, 215-231.

Cetin, K.O., Seed, R.B., Moss, R.S., Der Kiureghian, A.K., Tokimatsu K., Harder L.F., Kayen, R. 2000. Field Performance Case Histories for SPT-Based Evaluation of Soil Liquefaction Triggering Hazard. *12th International Conference on Advances in Civil Engineering*

Darendeli, M. B. 2001. *Development of a new family of normalized modulus reduction and material damping curves*, University of Texas, Austin.

Dobry, R., Abdoun, T. 2015. 3th Ishihara Lecture: An investigation into why liquefaction charts work: A necessary step toward integrating the states of art and practice. *Soil Dynamics and Earthquake Engineering* **68**, 40-56.

Idriss, I.M, Boulanger, R. 2008. *Soil Liquefaction During Earthquakes*, Earthquake Engineering Research Institute, Oakland, CA.

Kramer, S.L., Greenfield, M.W. 2019. The use of numerical analysis in the interpretation of liquefaction case histories. *7th International Conference on Earthquake Engineering*

Labanda, N.A., Sottile, M.G., Cueto, I.A., Sfriso, A.O. 2021. Screening of seismic records to perform time-history dynamic analyses of tailings dams: A power-spectral based approach. *Soil Dynamics and Earthquake Engineering* **146**.

Oommen, T., Baise, L., Vogel, R. 2010. Validation and application of empirical liquefaction models. *Journal of Geotechnical and Geoenvironmental Engineering, ASCE* **136**, 1618-1633.

Plaxis 2023. *PLAXIS General Information Manual*, Plaxis – Bentley Systems, The Netherlands.

Robertson, P. 1998. Evaluating cyclic liquefaction potential using the cone penetration test. *Canadian geotechnical journal* **34**, 442-459.

Seed, H.B., Idriss, I.M. 1971. Simplified procedure for evaluating soil liquefaction potential. *Journal of the Soil Mechanics and Foundations Division* **97**, 1249-1273.

Sottile, M., Tasso, N., Sfriso, A. 2021. Evaluación de potencial de licuación por acción sísmica mediante el uso de modelación numérica. *XXV Congreso Argentino de Mecánica de Suelos e Ingeniería Geotécnica*

Vilhar, G., Brinkgreve R.B.J., Zampich, L. 2018. *PLAXIS: The PM4Sand model*, Netherlands.

Youd T.L., Idriss I.M., Andrus R.D., Arango I., Castro, G., Christian J.T., et al. 2001. Liquefaction resistance of soils: summary report from the 1996 NCEER and 1998 NCEER/NSF workshops on evaluation of liquefaction resistance of soils. *Journal of Geotechnical and Geoenvironmental Engineering, ASCE* **127**, 817-833.

Zhang, J., Wang, Y. 2021. An ensemble method to improve prediction of earthquake-induced soil liquefaction: a multi-dataset study. *Neural Computing and Applications* **33**, 1533-1546.

Ziotopolou, K., Boulanger, R. 2015. *PM4Sand (Version 3): A Sand Plasticity Model for Earthquake Engineering Applications*, Center for Geotechnical Modelling, Report UCD/CGM-15/01.